

Role of solvent for globular proteins in solution

Andrey Shiryayev, Daniel. L. Pagan, James. D. Gunton

Department of Physics, Lehigh University, Bethlehem, P.A., USA 18015

D. S. Rhen

Department of Materials Science,

University of Cambridge,

Cambridge, CB2 3QZ, UK

Avadh Saxena and Turab Lookman,

Theoretical Division, Los Alamos National Laboratory,

Los Alamos, NM 87545 USA

December 31, 2004

Abstract

The properties of the solvent affect the behavior of the solution. We propose a model that accounts for the contribution of the solvent free energy to the free energy of globular proteins in solution. For the case of an attractive square well potential, we obtain an exact mapping of the phase diagram of this model without solvent to the model that includes the solute-solvent contribution. In particular we find for appropriate choices of parameters upper critical points, lower critical points and even closed loops with both upper and lower critical points, similar to one found before [1]. In the general case of systems whose interactions are not attractive square wells, this mapping procedure can be a first approximation to understand the phase diagram in the presence of solvent. We also present simulation results for both the square well model and a modified Lennard-Jones model.

1 Introduction

In recent years there has been an enormous increase in the number of proteins that can be isolated, due to the rapid advances in biotechnology. However, the determination of the function of these proteins has been slowed by the difficulty of determining their crystal structure by standard X-ray crystallography. A major problem is that it is difficult to grow good quality protein crystals. Experiments have clearly shown that this crystallization depends sensitively on the physical factors of the initial solution of proteins. An important observation was made by George and Wilson [2], who showed that x-ray quality globular protein crystals only result when the second virial coefficient, B_2 , of the osmotic pressure of the protein in solution lies within a narrow range. This corresponds to a rather narrow temperature window. For large positive B_2 , crystallization does not occur on observable time scales, whereas for large negative B_2 , amorphous precipitation occurs. Rosenbaum, Zamora and Zukoski then showed [3] that crystallization of globular proteins could be explained as arising from attractive interactions whose range is small compared with the molecule's diameter (corresponding to the narrow window of B_2). In this case the gas-fluid coexistence curve is in a metastable region below the liquidus-solidus coexistence lines, terminating in a metastable critical point.

When a system undergoes a phase transition the change in the Gibbs free energy ΔG consists of two terms - an enthalpy change ΔH and an entropy change ΔS , with $\Delta G = \Delta H - T\Delta S$. The change in the Gibbs free energy must be negative in order for the transition to occur. The enthalpy change is negative because in the separated state the more dense phase has a larger number of contacts and therefore its contact energy is lower. However, the dense state has a lower entropy and its entropy change is also negative. These two terms compete and at low temperatures the free energy change due to particles going from the dilute phase to the dense phase is negative and phase separation occurs. However, above some temperature the entropy loss exceeds the enthalpy loss, so that the change in the Gibbs free energy is positive and phase separation does not occur.

The solvent can change this picture dramatically [4]. Consider the free energy change of the particle going from the dilute phase to the dense phase.

$$\Delta G = \Delta H_{solute} - T\Delta S_{solute} + \Delta H_{solvent} - T\Delta S_{solvent} \quad (1)$$

Here ΔH_{solute} is the enthalpy change of the particle between the dense and dilute phases, ΔS_{solute} is the entropy of the solute particle change, $\Delta H_{solvent}$ is the enthalpy change of the solvent and $\Delta S_{solvent}$ is the entropy change of the solvent. The first two terms on the right side of (1) behave exactly as described above. The last two terms, however can be either negative or positive.

As an example of this, consider water. Water has a large number of strong intermolecular hydrogen bonds in the bulk state. When one adds a hydrophobic particle to water, some of these bonds break. This leads to an increase in the entropy of water and to a decrease in its enthalpy. However, the further rearrangement of the water molecules around the solute particle leads to even stronger bonds, thereby decreasing solvent entropy and decreasing the solvent enthalpy. When particles aggregate the water molecules return to the original bulk state so the entropy and the enthalpy of the water increase to their original values[5, 6, 7, 8]. This is an example how the $\Delta S_{solvent}$ and the $\Delta H_{solvent}$ terms in (1) can be positive. If the sign of the total enthalpy and the total entropy change is positive, then decreasing temperature can lead to the opposite behavior, when the system tends to be separated above some temperature and uniform below. This leads to a lower critical point. This phenomenon has been experimentally observed in different systems [9, 10, 11, 12]. The most interesting example of a lower critical point in context of our work is the phase diagram of sickle hemoglobin, which is thought to have an upside down fluid fluid coexistence curve [13], as inferred from the observation of an upside down spinodal curve.

Below the lower critical point the water molecules build strong hydrogen bonds around solute particles preventing them from aggregating. As one increases the temperature the free energy decrease of the aggregating particles surpasses the free energy gain of the water and the system phase separates. If one increases the temperature further, the total entropy loss due to aggregation becomes larger than the total enthalpy loss, so the phase separation becomes less favorable again and above some upper critical temperature the system becomes uniform. Thus for the hydrophobic particles one can have both an upper and a lower critical point; in other words, the fluid-fluid phase diagram has the form of a *closed loop*. This can be the case for different protein-water solutions.

In this paper we present a simple model for the role of the solvent. We model the multicomponent protein-solvent system as a binary system in which the solute molecule is much bigger than the solvent.

We assume that the role of other components in the system are subsumed in the effective solute-solute interaction. The role of a salt, for example, is assumed simply to screen the charge on the proteins, inducing the effective inter particle attraction, whose strength is controlled by the salt concentration. This assumption permits us to predict three qualitatively different effects of the role of the solvent for globular proteins in solution, all of which are consistent with experimental observation [4, 14]. The first is a negative enthalpy and entropy of crystallization, which gives a normal liquid-solid line. Lysozyme is an example of this, as it has a negative enthalpy of crystallization, of the order of minus 75 kJ^{-1} . The second is a positive enthalpy of crystallization, which gives the upside down (retrograde) behavior of coexistence curves. This has been seen in hemoglobin C (CO-HbC), which has a high positive enthalpy of 155 kJ^{-1} of crystallization. This system exhibits a strong retrograde solubility dependence on temperature (figure 1). Another example of retrograde behavior is chymotrypsinogen A [15]. The third is a zero enthalpy of crystallization, which gives vertical coexistence curves. Apoferritin has an enthalpy of crystallization close to zero and has a solubility which is independent of temperature (vertical behavior in the temperature-solubility diagram).

We consider a situation in which the solute particle-particle interactions are described by a repulsive hard core together with an attractive interaction. For example, the interparticle potential might be described by the DLVO potential [16], which consists of a Debye-Hückel interaction and a van der Waals interaction. Other model potentials are the square well and modified Lennard-Jones models that have been used successfully in recent years to describe globular proteins in solution. If the attractive part is short-ranged then these effective potentials can qualitatively describe the canonical phase diagram of the globular protein solution. We can therefore consider that solvent contribution was accounted in these effective potentials and there is no need to add the solvent-solute interactions into potential. Examples of proteins that have canonical phase diagram are Lysozyme [17, 15] and γD -crystallin [18]. However for proteins that have completely different phase diagram (like apoferritin or HbS, HbC) these effective potentials fail to describe the phase diagram even qualitatively. In this case the solvent contribution wasn't successfully included into effective potential. The model presented in this paper is an attempt to account for the solvent effect to describe the phase diagrams of the proteins like apoferritin, HbS, HbC at least qualitatively.

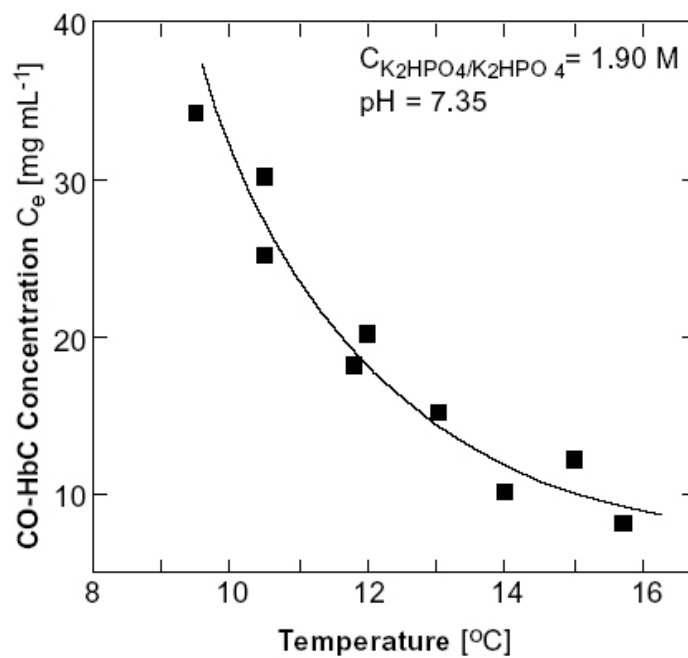


Figure 1: Solubility curve of CO HbC at conditions indicated at the plot. Points are the experimental results and the curve is fit using $\Delta H = 155kJ/mol$ Details of the fitting procedure can be found in [4].

The figure was nicely granted by P. G. Vekilov.

We then include a simplified solute-solvent interaction to the solute-solute interaction, which is similar to one used recently to describe hydrophobic interactions [1]. Our particular interest is globular proteins in solution, but our treatment in principle includes other systems.

The outline of the paper is as follows. Section 2 contains a description of our model, while section 3 contains a discussion of the particular case of a square well system with solvent. For this particular choice of solute-solute interaction, we are able to obtain the phase diagram of the square-well potential model **with** solvent contribution from the phase diagram of the square-well potential **without** solvent contribution. Section 4 discusses three cases of this mapping, for different choices of parameter values, that yield upper critical points, lower critical points, and closed loops, respectively. Section 5 contains a derivation of a modified Clausius-Clapeyron equation in the presence of the solvent, that takes into account the temperature dependence of the effective interaction potential. Section 6 contains the results of a simulation of a modified Lennard-Jones model plus solvent. The modified Lennard-Jones model was originally introduced to describe the phase diagram and nucleation rates for globular proteins in solution [19]. We show that for a particular choice of parameter values the solvent produces a fluid-fluid coexistence curve with a lower critical point. The liquid-solid coexistence lines for this model are also shown. Finally, section 7 contains a brief conclusion.

2 Simple model for solvent-solute interaction

In this section we will derive a phenomenological model that describes the influence of the solvent on a system of interacting protein particles. Consider a system of protein particles interacting via a short ranged pairwise potential $U(\vec{r}_{ij})$. The total energy of such a system is

$$U_0(\mathbf{r}^N) = \frac{1}{2} \sum_{i \neq j} U_0(|\mathbf{r}_i - \mathbf{r}_j|) \quad (2)$$

where the subscript 0 denotes the potential energy in the absence of the solvent. The corresponding Helmholtz free energy $F_0(N, V, T)$ of the system is

$$F_0(N, V, T) = -k_B T \ln \left(\frac{1}{\Lambda^{3N} N!} \int d\mathbf{r}^N \exp(-\beta U_0(\mathbf{r}^N)) \right) \quad (3)$$

where N is the number of particles in a volume V , Λ is the thermal de Broglie wavelength, \mathbf{r} the coordinates of the particles and k_B is a Boltzman constant. To take into account the effect of the solvent

on this system, we note that a particular solvent molecule can be either in the bulk or in a "shell" region around a protein particle (see Fig. 2). We define the energy and entropy (in units of k_B) differences between these two states to be ϵ_w and Δs_w , respectively. In general these quantities depend on the temperature [20, 1], i.e. $\epsilon_w = \epsilon_w(T)$, $\Delta s_w = \Delta s_w(T)$. Thus the free energy difference between a solvent molecule in the bulk and in the shell is $\Delta f = \epsilon_w - k_B T \Delta s_w$. The total energy of the protein-water system therefore is

$$U = U_0 + \sum_{i=1}^N (\epsilon_w - k_B T \Delta s_w) n_w^{(i)}(\mathbf{r}^N) \quad (4)$$

where $n_w^{(i)}$ is the number of water molecules around the i^{th} particle. We now assume that this number is proportional to the available area on the protein molecule surface and approximate this area as proportional to the maximum possible number of contacts of the protein molecule with other protein molecules. That is, the available energy is proportional to n_c minus the actual number of contacts $n_p^{(i)}$.

$$n_w^{(i)}(\mathbf{r}^N) \propto n_c - n_p^{(i)}(\mathbf{r}^N) \quad (5)$$

We absorb the proportionality coefficient into ϵ_w and Δs_w . Next, define two particles to be in contact when the distance between their centers of mass is less than some value $\lambda_c \sigma$ and greater than σ , where σ is the hard core diameter. Define the function $\gamma(|\mathbf{r}_i - \mathbf{r}_j|)$ to be equal to one if the distance between particles i and j is less than $\lambda_c \sigma$, but greater than σ and is zero otherwise. If the distance between the particles is less than their hard core diameter, the total energy of the system is infinite, which is the value of $U_0(|\mathbf{r}_i - \mathbf{r}_j| < \sigma)$, so one can define $\gamma(|\mathbf{r}_i - \mathbf{r}_j| < \sigma) = 0$ at that distance. The number of contacts for the i^{th} particle is then given by

$$n_p^{(i)} = \sum_{i \neq j} \gamma(|\mathbf{r}_i - \mathbf{r}_j|) \quad (6)$$

Combining equations (4), (5) and (6), we find that the total energy of the system is

$$U(\mathbf{r}^N) = \frac{1}{2} \sum_{i \neq j} U_0(|\mathbf{r}_i - \mathbf{r}_j|) + (\epsilon_w - k_B T \Delta s_w) \left(N n_c - \sum_{i \neq j} \gamma(|\mathbf{r}_i - \mathbf{r}_j|) \right) \quad (7)$$

We can combine the first and the last terms on the right hand side and define a modified intermolecular interaction parameter

$$U(|\mathbf{r}_i - \mathbf{r}_j|) = U_0(|\mathbf{r}_i - \mathbf{r}_j|) - 2(\epsilon_w - k_B T \Delta s_w) \gamma(|\mathbf{r}_i - \mathbf{r}_j|) \quad (8)$$

In summary, our model assumes that a water molecule can be either in the bulk or close to the protein particle (shell); the number of water molecules near the particle is proportional to the available area on the surface of the particle; the available area on the protein surface is proportional to the maximum possible number of protein-protein contacts minus the actual number of contacts.

3 Square well system with solvent

3.1 Implementation of the general theory

In order to simplify this expression for the energy, we consider a system with a repulsive hard core and an attractive square-well (SW) potential, whose range of attraction is λ_c . We can write U_0 in the form of $U_0 = -1/2 \sum_{i=1}^N \epsilon_0 n_p^{(i)}$, where ϵ_0 is the well depth. The total energy of such a system is

$$U(\mathbf{r}^N) = -\frac{1}{2} \sum_{i=1}^N (\epsilon_0 + 2\epsilon_w - 2k_B T \Delta s_w) n_p^{(i)} + (\epsilon_w - k_B T \Delta s_w) N n_c \quad (9)$$

The first term on the right hand side is just the energy of the square-well potential with the well depth $\tilde{\epsilon} = \epsilon_0 + 2\epsilon_w - 2k_B T \Delta s_w$. This simplification allows us to map the phase diagram of this square-well potential model **with** solvent contribution onto the phase diagram of the square-well potential **without** solvent contribution. Denote the free energy of the square-well system with well depth ϵ as $F_0(N, V, T; \epsilon)$. The second term on the right hand side of (9) does not depend on the position of the particles. Therefore the free energy of the SW system **with** solvent

$$F(N, V, T) = F_0(N, V, T; \tilde{\epsilon}) + (\epsilon_w - k_B T \Delta s_w) N n_c \quad (10)$$

The free energy density of the system is

$$f(\rho, T) = f_0(\rho, T; \tilde{\epsilon}) + \rho n_c (\epsilon_w - k_B T \Delta s_w) \quad (11)$$

where f_0 is the free energy density of the square-well system (without solvent). Denote μ_0 and ω_0 as the chemical potential and grand canonical free energy density respectively. In this case $\mu_0 = \partial f_0 / \partial \rho$ and $\omega_0 = f_0 - \mu_0 \rho$. To obtain the phase diagram for the square-well system one needs to solve the phase coexistence conditions $\mu_0(\rho_1, T) = \mu_0(\rho_2, T)$ and $\omega_0(\rho_1, T) = \omega_0(\rho_2, T)$. Suppose that we have obtained this phase diagram in some way (numerically, for example). The square-well coexistence curve has the

following functional form

$$\frac{kT_{coex}}{\epsilon} = \tau(\rho) \quad (12)$$

To obtain the phase diagram of a square well system **with** the solvent we should write the chemical potential and grand canonical free energy in terms of μ_0 and ω_0 .

$$\begin{aligned} \mu(\rho, T) &= \mu_0(\rho, T; \tilde{\epsilon}) + n_c(\epsilon_w - k_B T \Delta s_w) \\ \omega(\rho, T) &= \omega_0(\rho, T; \tilde{\epsilon}) \end{aligned} \quad (13)$$

As we can see the phase diagram for the protein solvent system maps to the square well phase diagram with the well depth $\epsilon_0 + 2\epsilon_w - 2k_B T \Delta s_w$:

$$\frac{kT_{coex}}{(\epsilon_0 + 2\epsilon_w - 2k_B T_{coex} \Delta s_w)} = \tau(\rho) \quad (14)$$

Assuming that ϵ_w and Δs_w do not depend on temperature, the relationship between the phase diagrams for these two models is given by

$$k_B T_{coex} = \frac{(\epsilon_0 + 2\epsilon_w)}{(1 + 2\Delta s_w \tau(\rho))} \tau(\rho) \quad (15)$$

In summary, we are able to obtain the phase diagram for an interacting protein system that includes the effect of solvent in terms of the interacting protein system without solvent, assuming that the protein-water attractive interactions are given by a square well potential; that the range of the protein-water interaction is equal to the range of the protein-protein interaction $\lambda = \lambda_c$ and that the parameters ϵ_w and Δs_w are constants.

4 Upper and lower critical points and closed loops

4.1 Upper and lower critical points

In this section we consider examples of the phase diagram mapping for the square well model with solvent. Let $\tau(\rho)$ in (12) be a fluid-fluid coexistence curve. The critical point can be determined by the following condition

$$\frac{\partial kT_{coex}}{\partial \rho_{coex}} = 0 \quad (16)$$

If we define the left hand side of (14) as $G(kT)$ then

$$\partial kT_{coex}/\partial \rho_{coex} = \frac{d\tau(\rho)/d\rho}{dG(kT)/dkT}$$

This means that the critical density of the modified system is the same as the critical density of the original square well system. The second derivative shows whether there is an upper or lower critical point. Taking into account that $d\tau/d\rho = 0$ at the critical point, we obtain

$$\frac{\partial^2 kT}{\partial \rho^2} = \frac{d^2\tau/d\rho^2}{dG/dkT}_{crit} \quad (17)$$

The original square well model has an upper critical point, so $d^2\tau(\rho_{cr})/d\rho^2 < 0$. Therefore the sign of the denominator determines the type of the critical point. If $dG(kT_{cr})/dkT > 0$ then there is an upper critical point.

In our simplified model with constant ϵ_w and Δs_w we can calculate dG/dkT explicitly $dG/dkT = (\epsilon_0 + 2\epsilon_w)/(\bar{\epsilon}^2)$. This gives the first condition for upper or lower critical points. The temperature in (15) should be positive. This gives the second condition required for having upper or lower critical points.

$$\epsilon_w > -\epsilon_0/2, \Delta s_w > \epsilon_0/2kT_{cr}^0 - \text{upper critical point} \quad (18)$$

$$\epsilon_w < -\epsilon_0/2, \Delta s_w < \epsilon_0/2kT_{cr}^0 - \text{lower critical point} \quad (19)$$

where T_{cr}^0 is the critical temperature of the original system without solvent.

4.2 Closed loop phase diagram

One of the possible fluid-fluid coexistence curves is a closed loop [1] with both upper and lower critical points. In order to obtain this behavior from our model we must have temperature dependent ϵ_w and Δs_w . We use the four level Muller, Lee, and Graziano (MLG) model of water [21, 22, 1] to obtain $\epsilon_w(kT)$ and $\Delta s_w(kT)$. In this model water molecules can be either in disordered (broken hydrogen bonds) or ordered states. When the protein particles are added, each state of a water molecule splits into shell and bulk states. Thus we have a four level model (Fig. 2). The values of the energy levels and degeneracies used in [1] are following : $E_{os} = -2$, $E_{ob} = -1$, $E_{db} = 1$, $E_{ds} = 1.8$, $q_{os} = 1$, $q_{ob} = 10$, $q_{db} = 40$ and $q_{ds} = 49$. Moelbert and De Los Rios [1] considered a lattice model using the four level approximation and found by Monte Carlo simulation a fluid-fluid coexistence line in the form of a closed loop

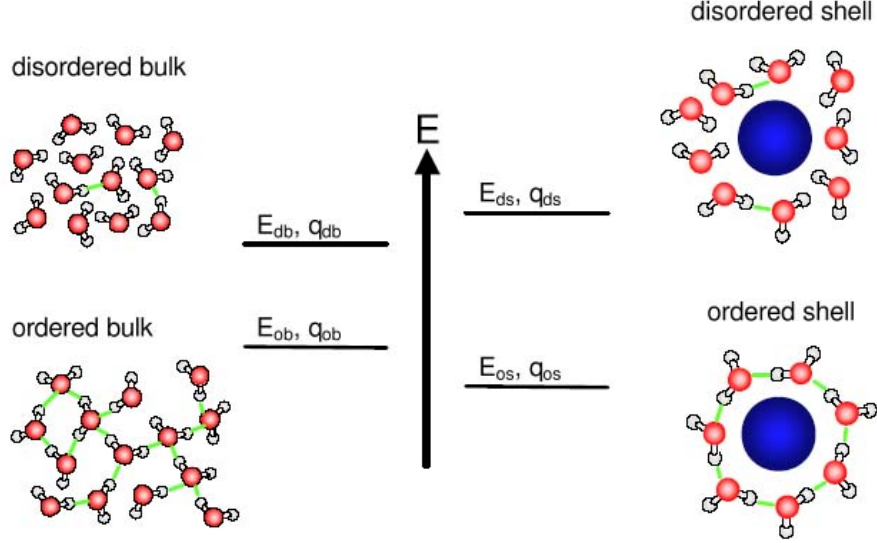


Figure 2: Energy levels for the MLG model for water. The configurations of the different states are shown schematically. The figure was nicely granted by S. Moelbert [23].

Using the above values of energies and degeneracies we can calculate the energy levels of the shell and bulk states:

$$E_s = \frac{E_{os} + E_{ds}e^{-\beta\Delta E_s}}{1 + e^{-\beta\Delta E_s}} \quad (20)$$

$$E_b = \frac{E_{ob} + E_{db}e^{-\beta\Delta E_b}}{1 + e^{-\beta\Delta E_b}} \quad (21)$$

In the same way we determine the values of the entropies for the bulk and shell states:

$$\frac{1}{k_B} S_s = \ln\left(\frac{q_{os} + q_{ds}e^{-\beta\Delta E_s}}{1 + e^{-\beta\Delta E_s}}\right) \quad (22)$$

$$\frac{1}{k_B} S_b = \ln\left(\frac{q_{ob} + q_{db}e^{-\beta\Delta E_b}}{1 + e^{-\beta\Delta E_b}}\right) \quad (23)$$

where $\Delta E_s = E_{ds} - E_{os}$ and $\Delta E_b = E_{db} - E_{ob}$. The parameters of our model ϵ_w and Δs_w are the differences of the energies and entropies in the bulk and shell states respectively,

$$\epsilon_w(kT) = E_s - E_b \quad (24)$$

$$\Delta s_w(kT) = S_s - S_b \quad (25)$$

Substituting (24) and (25) into (14) we can numerically map the square well phase diagram onto the MLJ-model phase diagram. Figure 3 shows the dependence of the left hand side of (14) versus the

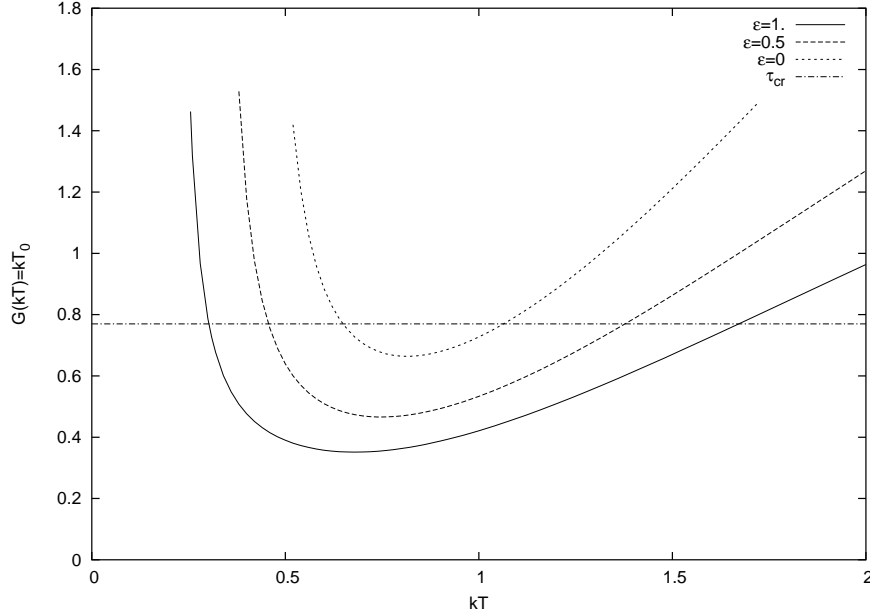


Figure 3: The dependence of the left hand side of (14) on the temperature for the MLG-type system (Mapping Curve) for 3 values of the protein-protein interaction energy. The horizontal dashed line shows the critical temperature of the original square well system (without solvent). All curves intersects the critical temperature of the system without solvent twice. This means that the MLG system in these cases has two critical points - one is the lower critical point (the slope of the curve is negative), the other is the upper critical point (the slope of the curve is positive). The phase diagram contains closed loop containing these two critical points. The parameters for the curves are the following $E_{os} = -2$, $E_{ob} = -1$, $E_{db} = 1$, $E_{ds} = 1.8$, $q_{os} = 1$, $q_{ob} = 10$, $q_{db} = 40$, $q_{ds} = 49$

temperature of the system (mapping curve) in the presence of solvent for three different values of the protein-protein interaction strength. The horizontal line in fig. 3 represents the critical temperature of the original square-well system without solvent. The intersection of the mapping curve with the horizontal line is the critical temperature of the system in the presence of solvent. For each curve in fig. 3 there are two intersections with the horizontal line. Therefore the mapping procedure yields two critical points - one lower and one upper. The mapping of the entire original coexistence curve gives a closed loop type phase diagram for the MLG-type system.

Using (20) - (23) we can obtain the low and high temperature values of ϵ_w and Δs_w . This permits

us to determine the upper and lower critical points. In the low temperature limit

$$\epsilon_w(0) = E_{os} - E_{ob} \quad (26)$$

$$\Delta s_w(0) = \ln(q_{os}/q_{ob})$$

and in the high temperature limit:

$$\epsilon_w(\infty) = \frac{E_{os} + E_{ds}}{2} - \frac{E_{ob} + E_{db}}{2} \quad (27)$$

$$\Delta s_w(\infty) = \ln\left(\frac{q_{os} + q_{ds}}{q_{ob} + q_{db}}\right)$$

One necessary (but not sufficient) condition to have both upper and lower critical points is (26) to satisfy conditions (19) and (27) to satisfy (18). The second condition would require that the minimum of the mapping curve is lower than the critical temperature of the original system without solvent (fig. 3).

4.3 The case in which the range of the solute-solute interactions, λ , differs from the solute-solvent interactions, λ_s

So far we have considered a special case in which the range of the solute-solute interaction is equal to the that of the shell region. In general this is not the case. In this section we develop an approximate mapping for such systems. We use Brilliantov's result [24] for the mean field relations between the critical temperature and critical density:

$$\frac{kT_c}{v_0} = \rho_c \left[z_0 + \frac{u_3}{2u_4} \right]_{CP} = h(\rho_c) \quad (28)$$

where v_0

$$v_0 = \int v(\mathbf{r}) d\mathbf{r} \quad (29)$$

is the zeroth order moment of the attractive part $v(\mathbf{r})$ of the potential. The terms inside the brackets on the right hand side of (28) are explained in [24]. This mean-field approximation has different precision for different interactions and even for the same interaction with different parameters. Division of the potential into the repulsive and attractive parts adds more freedom to obtaining parameter v_0 (29)¹, which also reduce quantitative precision. The assumption made in this section is that the critical density

¹One of the methods to choose the form of the attractive part of potential is to set pair-correlation function $g(r)$ equal to zero for r less than hard core diameter [25]

is the same for the systems with and without solvent. This is approximately true for $\lambda_s < \lambda = 1.25$, where the critical density is about 0.4. For higher values of λ this assumption fails. The analysis given in this section therefore can provide only qualitative understanding of the behavior of the critical temperature for different λ_s .

What is important is that the right hand side of (28) depends only on the isothermal compressibility and its derivatives with respect to density of the hard sphere system [24]. So for our purpose this is just some function of the density and independent of temperature.

The square well system in the absence of solvent has v_0 equal to

$$v_0 = -\frac{4\pi\sigma^3}{3}(\lambda^3 - 1)\epsilon_0 \quad (30)$$

where ϵ_0 is the well depth of the particle particle interaction. For the system in the presence of the solvent v_0 has the form:

$$v_0^s = -\frac{4\pi\sigma^3}{3}(\lambda^3 - 1)\epsilon_0 - 2(\epsilon_w - kT_c^s \Delta s_w) \frac{4\pi\sigma^3}{3}(\lambda_s^3 - 1) = v_0 \left(\frac{\epsilon_0}{\epsilon} + \frac{2(\epsilon_w - kT_c^s \Delta s_w)}{\epsilon} \frac{\lambda_s^3 - 1}{\lambda^3 - 1} \right) \quad (31)$$

Substituting v_0 and v_0^s into (28) and assuming that the critical density doesn't change we get the relationship between the critical temperature of the system without solvent and the critical temperature of the system with solvent:

$$kT_c^s = kT_c \left[\frac{\epsilon_0}{\epsilon} + \frac{2(\epsilon_w - kT_c^s \Delta s_w)}{\epsilon} \frac{\lambda_s^3 - 1}{\lambda^3 - 1} \right] \quad (32)$$

Solving (32) for the kT_c^s we get the mapping relationship similar to (15) but for the critical temperature only:

$$k_B T_{coex} = \frac{(\epsilon_0 + 2\epsilon_w \frac{\lambda_s^3 - 1}{\lambda^3 - 1})}{(1 + 2\Delta s_w \tau(\rho_c) \frac{\lambda_s^3 - 1}{\lambda^3 - 1})} \tau(\rho_c) \quad (33)$$

For the special case λ_s equal to λ this becomes (15) with $\tau_c = kT_c/\epsilon$. The main difference is that the relationship (15) is for all temperatures, while the (33) is only for the critical point. Let λ_s^0 be the value of λ_s at which the denominator on the right hand side of (33) vanishes. For $\lambda_s < \lambda_s^0$ the system has an upper critical point behavior. For $\lambda_s > \lambda_s^0$ the system has a lower critical point behavior.

Using (32) we can approximately map the phase diagram. In this case we can introduce the effective

solvent parameters

$$\begin{aligned}\epsilon_w^{eff} &= \epsilon_w \frac{\lambda_s^3 - 1}{\lambda^3 - 1} \\ \Delta s_w^{eff} &= \Delta s_w \frac{\lambda_s^3 - 1}{\lambda^3 - 1}\end{aligned}$$

These effective parameters correspond to the solute-solvent system with an effective shell size $\lambda_s^{eff} = \lambda$, with a zeroth moment v_0 equal to v_0^s . So we approximately change the system with solvent and $\lambda_s \neq \lambda$ by the system with solvent and effective parameters ϵ_w^{eff} and Δs_w^{eff} with $\lambda_s^{eff} = \lambda$. This allows us to perform a mapping of the SW system phase diagram onto the effective system with solvent phase diagram using (32). We can consider the latter as the qualitative behavior of the system of interest.

5 Modification of the Clausius-Clapeyron equation in the presence of the solvent

Now we consider a liquid-solid coexistence in the presence of the solvent. To determine the solid-liquid coexistence curve we use Gibbs-Duhem integration proposed by Kofke [26, 27]. This method is based on the integration of the Clausius-Clapeyron equation:

$$\frac{dP}{dT} = \frac{\Delta S}{\Delta V} \quad (34)$$

where ΔS and ΔV are the entropy and volume differences between solid and liquid phases, respectively. The derivative is taken along the coexistence curve. In the absence of the solvent this equation leads to the following form:

$$\frac{dP}{dT} = \frac{\Delta e + P\Delta v}{T\Delta v} \quad (35)$$

where $\Delta e = e_s - e_l$ and Δv are the differences in the energy and volume per particle in the solid and liquid phases respectively.

When we have the model with a solvent contribution given by (7) or (9), the interaction potential is temperature dependent. Therefore one must modify the (35) to take this temperature dependence into account. We start from the origins of the (34). For the coexistent phases the difference of the Gibbs free

energies is zero $\Delta G = G_s - G_l = 0$. Thus the derivative is taken at the conditions of $\Delta G = 0$

$$\left(\frac{dP}{dT}\right)_{\Delta G=0} = -\frac{(\partial\Delta G/\partial T)_{NP}}{(\partial\Delta G/\partial P)_{NT}} = \frac{\Delta S}{\Delta V} \quad (36)$$

To get ΔS we substitute the Gibbs partition function into $S = -\partial G/\partial T$, where $G = -k_B T \ln \Xi(N, P, T)$, and

$$\Xi(N, P, T) = C \int dV d\mathbf{r}^N \exp[-\beta(U(\mathbf{r}^N, T) + PV)] \quad (37)$$

The derivative of the Gibbs free energy with respect to temperature then is

$$S = k \ln \Xi(N, P, T) + \frac{kT}{\Xi(N, P, T)} \int \left(\frac{U + PV}{kT^2} - \frac{\partial U}{\partial T} \frac{1}{kT} \right) e^{-\beta(U(\mathbf{r}^N, T) + PV)} dV d\mathbf{r}^N$$

which leads to

$$TS = -G + \langle U \rangle + P \langle V \rangle - T \langle \partial U / \partial T \rangle \quad (38)$$

Substituting this expression for the entropy into (34) we obtain the following modification of the Clausius-Clapeyron equation

$$\frac{dP}{dT} = \frac{\Delta e + P\Delta v - T\Delta\partial e}{T\Delta v} \quad (39)$$

where $\partial e = \langle \partial U / \partial T \rangle / N$.

When the Hamiltonian of the system consists of two body interactions between particles, the temperature is determined by the average kinetic energy and a temperature dependent microscopic Hamiltonian doesn't make much sense. In this case, however, we have a system of solute particles in a solvent environment. A rearrangement of the solute particles leads to a rearrangement of solvent particles. The entropy of the system consists of two parts: the entropy of the protein particles and the entropy of the solvent molecules. Since in our model we don't consider separate solvent molecules, but rather just average their contribution, the effective interaction (8) has the temperature dependent term due to having integrated out the solvent degrees of freedom. This gives us the temperature dependent effective interaction. The last term in equation (38) can be considered as the solvent entropy contribution.

In the case of the square well protein-protein interactions, we can use the potential (9). The derivative of this potential with respect to the temperature is

$$\frac{\partial U}{\partial T} = - \left(\frac{\partial \epsilon_w}{\partial T} - k_B T \frac{\partial \Delta s_w}{\partial T} - k_B \Delta s_w \right) \left(\sum_{i=1}^N n_p^{(i)} - N n_c \right) \quad (40)$$

The $-Nn_c$ term in (40) cancels when we calculate the difference between solid and liquid phases. The average of this derivative per particle gives $\partial e = \delta(\langle n_p \rangle - n_c)$, where δ is the expression in the first parenthesis in (40) and $\langle n_p \rangle$ is the average number of protein-protein contacts. Using 9 we can relate the average number of contacts to the average energy. The difference between the average number of contacts in the solid and liquid phases is then related to the Δe :

$$\Delta \langle n_p \rangle = -\frac{2\Delta e}{\epsilon + 2\epsilon_w - 2k_B T \Delta s_w} \quad (41)$$

The difference of ∂e between two phases is therefore

$$\Delta \partial e = -\frac{2\delta \Delta e}{\epsilon + 2\epsilon_w - 2k_B T \Delta s_w} \quad (42)$$

Substituting (42) into (39) we obtain the final expression for the Clausius-Clapeyron equation for the square-well model with solvent

$$\frac{dP}{dT} = \left(\frac{\epsilon + 2\epsilon_w - 2\frac{\partial \epsilon_w}{\partial T} + 2k_B T \frac{\partial \Delta s_w}{\partial T}}{\epsilon + 2\epsilon_w - 2k_B T \Delta s_w} \Delta e + P \Delta v \right) \frac{1}{T \Delta v} \quad (43)$$

In the case of a system in which the solvent-solute interactions are not given by a square well potential, we have

$$\frac{dP}{dT} = \left(\Delta e + P \Delta v - 2 \left[\frac{\partial \epsilon_w}{\partial T} - k_B T \frac{\partial \Delta s_w}{\partial T} - k_B \Delta s_w \right] \Delta e^{SW} \right) \frac{1}{T \Delta v} \quad (44)$$

In equation (35) Δe , and Δv are negative. The right hand side is therefore positive and the coexistent pressure increases with increasing temperature. In equation (44) Δe and Δv are again negative, but the term in parenthesis can be either negative or positive; therefore for some cases the coexistent pressure can decrease as we increase the temperature. This effect is similar to the upside-down fluid-fluid coexistence curve and is due to the entropy contribution from the solvent. While the difference between the solid and the liquid of the entropy is generally negative (the solid state is more ordered), the total solvent plus solute entropy difference can be positive. This means that the entropy increase of the solvent during protein crystallization due to the decrease of the contact number is greater than the entropy decrease of the solute. Therefore the numerator in (34) can be positive for some solvent parameters. At constant temperature $\Delta S = \Delta H/T$. Thus this solvent model can reflect three different cases experimentally observed by Vekilov [4]. One is a negative enthalpy and entropy of crystallization, which gives the normal liquid-solid line. Another is a positive enthalpy of crystallization, which gives the upside down

behavior of coexistence curves. The third is a zero enthalpy of crystallization, which gives the vertical coexistence curves.

6 Numerical results for the solvent model

6.1 Summary of the mapping procedure and results for the square well system

In this section we summarize the algorithm of the mapping of the canonical square well (SW) phase diagram onto the diagram of the square well system in the presence of the solvent. The range of particle-particle interactions and the range of the particle-solvent interactions is considered to be the same. For the illustration we use the SW system with $\lambda = 1.25$. Correspondingly $\lambda_s = \lambda = 1.25$. The phase diagram of the system without solvent is shown in the fig. 4. The temperature of the system *without* solvent we denote as τ in order to not to confuse it with the temperature of the system *with* solvent, which is still denoted as kT .

The dependence of the left hand side of (14) on the temperature of the system with solvent (kT in equation (14)) we will call the *mapping curve*. Now we construct the phase diagram of the system with the solvent. The mapping curve plays an important role in this construction process. Figure 5 shows the mapping procedure in detail. First we take the original phase diagram of the square well model(fig. 5A). Second, choose some temperature τ_1 and invert the mapping curve (fig. 5B) to obtain the corresponding temperature of the system with the solvent². Coexistent densities (ρ_1 and ρ_4 in the fig. 5) corresponding to the temperature τ_1 are also the coexistent densities of the system with solvent at a temperature kT_1 . Now choose another temperature τ_2 , invert it, using the mapping curve, to kT_2 and use densities ρ_2 and ρ_3 (fig. 5) as the coexistent densities at kT_2 for the system with solvent. By continuing this process we obtain the phase diagram for the system with solvent (figure 6). As one can see, this has a lower critical point and in general an upside down coexistence curve as compared with fig. 4. The interesting feature

²Note that for constant ϵ_w and Δs_w this inversion has an analytical solution (15). However for temperature dependent ϵ_w and Δs_w as in the case of the closed loop like phase diagram, we have to invert the mapping curve numerically.

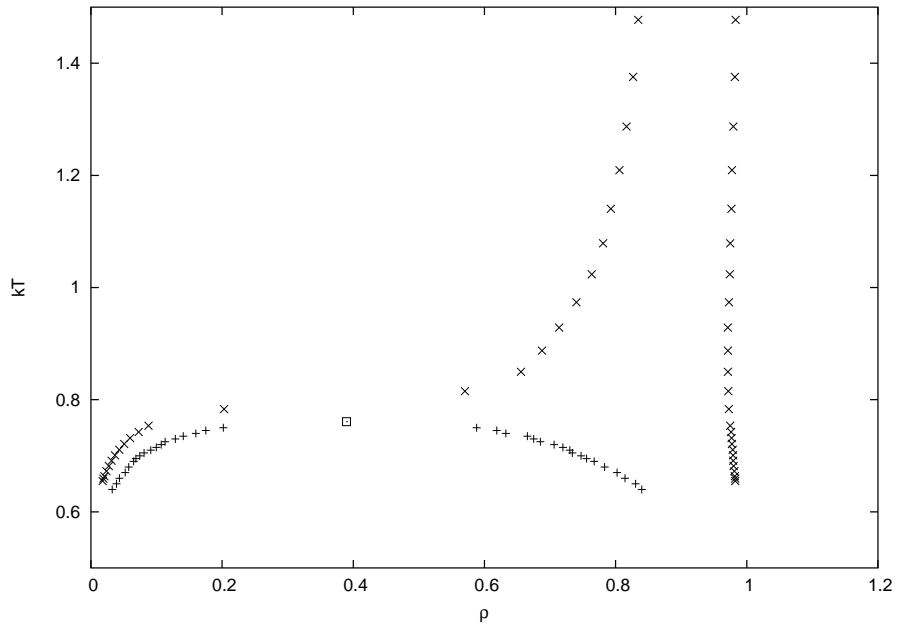


Figure 4: Phase diagram of the square well model with $\lambda = 1.25$. Here 'x' denotes liquid-solidus line; '+' denotes fluid-fluid coexistence. The fluid-fluid coexistence line was obtained using the Gibbs ensemble method with $N = 600$ and $V = 1500$. The liquid-solid coexistence line was obtained using thermodynamic integration and Gibbs-Duhem integration techniques. Open square shows the position of the critical point.

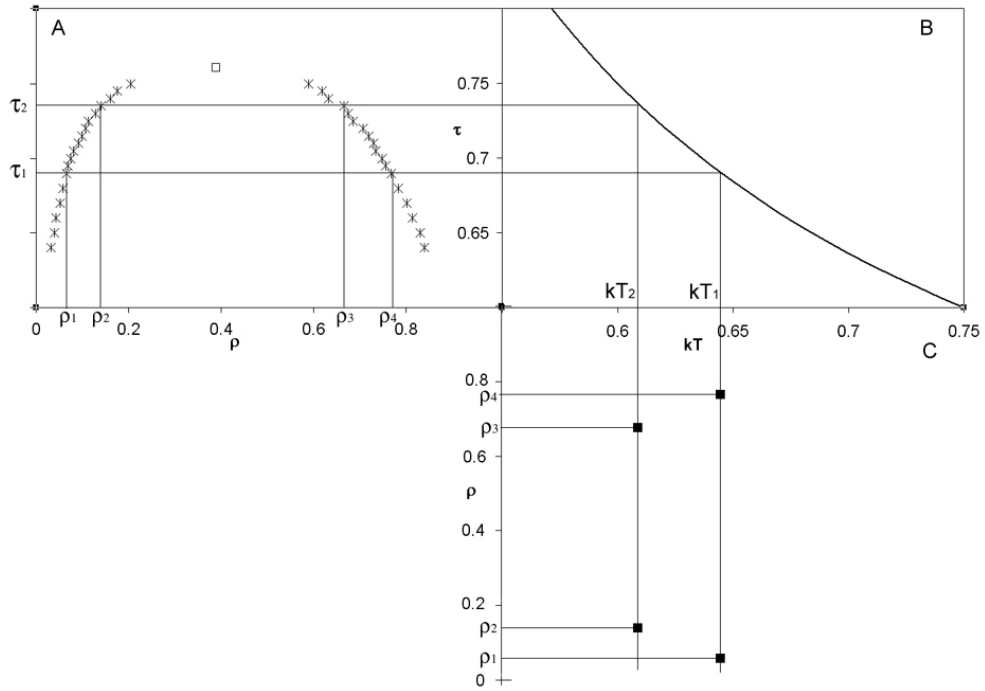


Figure 5: Mapping scheme. **A.** The fluid-fluid coexistence line for the square well model in the absence of solvent (same as on fig. 4). **B.** The mapping curve for $\epsilon_w = -1$ and $\Delta s_w = -1.5$. **C.** Results of the mapping. Filled squares are the points on the corresponding phase diagram for the square well model with solvent. See text for more description.

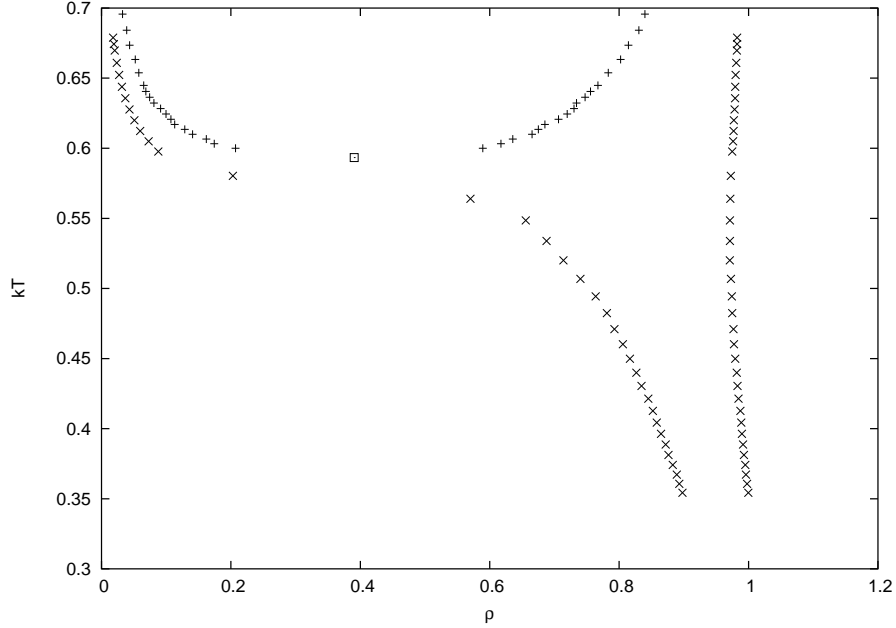


Figure 6: The phase diagram of the square well system with the solvent parameters $\epsilon_w = -1$ and $\Delta s_w = -1.5$, obtained by the procedure shown in figure 5. 'x' denotes liquid-solidus line; '+' denotes fluid-fluid coexistence.

of this phase diagram is that at a temperature equal to

$$kT_{HS} = \frac{\epsilon_0 + 2\epsilon_w}{2\Delta s_w} \quad (45)$$

the effective depth of the square well becomes zero and the particles behave as hard spheres, with the corresponding coexistent densities equal to the hard spheres case. In the figure 6 $kT_{HS} = 1/3$.

The next step is to invert the mapping curves shown in the figure 3. For this purpose we have to solve numerically equation (14) with parameters given by (20) - (23). Figure 7 shows three fluid-fluid coexistence curves corresponding to the three mapping curves shown on fig. 3. One can see that indeed the phase diagrams have the form of closed loops. This is because each temperature τ of the system without solvent corresponds to two temperatures kT_1 and kT_2 for the system with solvent. This can be understood from consideration of the MLG energy level model (fig. 2). At low temperatures the solvent molecules mostly occupy the lowest level, corresponding to the ordered shell. This state corresponds to the uniform distribution of the solute particles surrounded by the structures of solvent molecules. At high temperatures the solvent molecules mostly occupy the top energy level, which corresponds to the

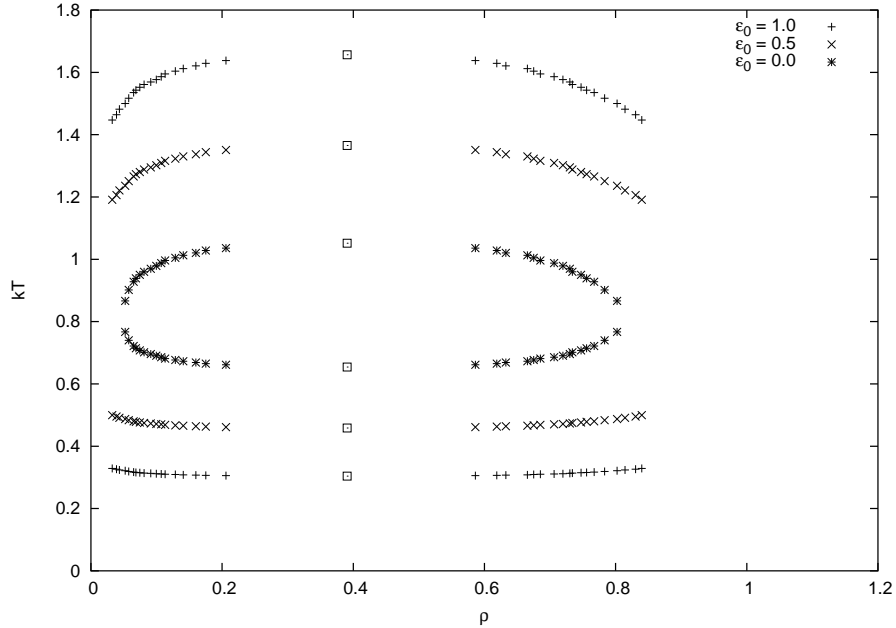


Figure 7: Fluid-fluid coexistence curves in the form of closed loop for the different protein-protein interaction strength ϵ_0 . The choice of solvent parameters is determined by equations (20) - (25). The case with $\epsilon_0 = 0$ qualitatively corresponds to the situation described in [1] where two proteins interact as hard spheres (on lattice).

disordered shell. So the system again tends to be in the uniform state, but now the solvent surrounding the solute particles is disordered. At intermediate temperature the system tends to occupy the bulk energy levels, which favors the phase separation. This is the property of the MLG model that reflects the picture described in the introduction.

The mapping curves shown in the figure 3 produce the closed loop like fluid-fluid coexistence curves. Figure 8 shows the behavior of the liquid-solid line in this case. The liquid-solid line also displays a behavior similar to the fluid fluid coexistence line. We are unaware of any experimental observations of such a liquid-solid coexistence behavior and do not know whether it is simply an artifact of our particular model.

6.2 Numerical results for the MLJ system in the presence of solvent

In this section consider the effect of solvent on particles interacting via a modified Lennard-Jones (MLJ) potential given by

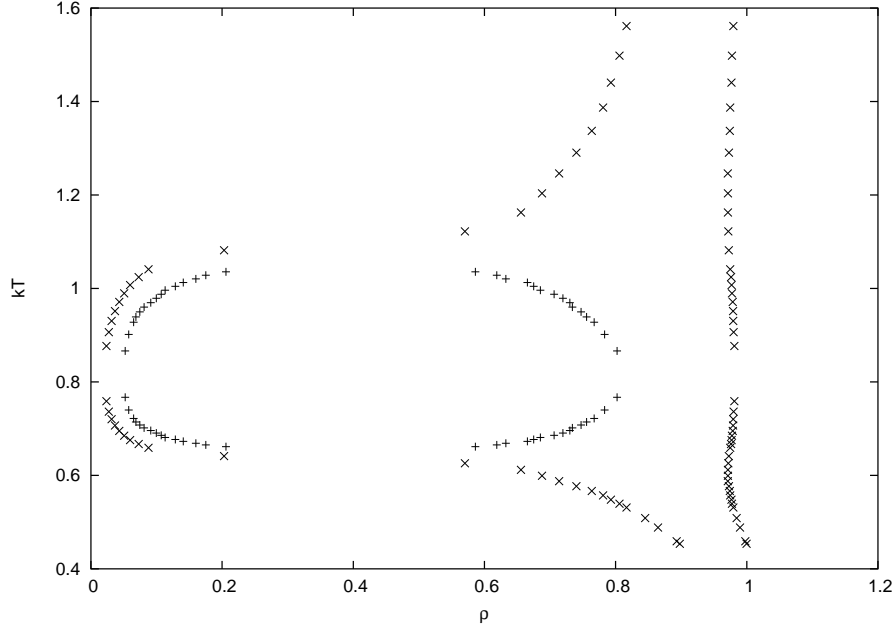


Figure 8: The fluid-fluid coexistence line as well as the solid-liquid coexistence line for the protein-protein interaction strength $\epsilon_0 = 0$ for the choice of parameters determined by equations (20) - (25).

$$V(r) = \begin{cases} \infty, & r < \sigma \\ \frac{4\epsilon}{\alpha^2} \left(\frac{1}{[(r/\sigma)^2 - 1]^6} - \frac{\alpha}{[(r/\sigma)^2 - 1]^3} \right) & r \geq \sigma. \end{cases} \quad (46)$$

It has been shown that at the critical point the nucleation rate is many orders of magnitude greater than at other points in the phase diagram. This suggests that the nucleation of protein particles can be achieved near the critical point. The model has been well studied and its critical point accurately determined.

For the case of the MLJ model, we again choose to use a solvent-solute interaction range, λ_s , that is equal to the protein-protein particle interaction range. Because the particles interacting via this potential have an effective hard-core diameter, care must be taken such that we choose an appropriate value for λ_s . We calculate the effective hard-core diameter using

$$\sigma_{eff} = \int_0^\infty dr [1 - \exp(-V_{rep}/k_B T)], \quad (47)$$

where V_{rep} is the repulsive part of the potential. The range over which the particles interact is controlled by the parameter α in 6.2. We choose $\alpha = 50$ as in other studies. It has been shown that for $\alpha = 50$,

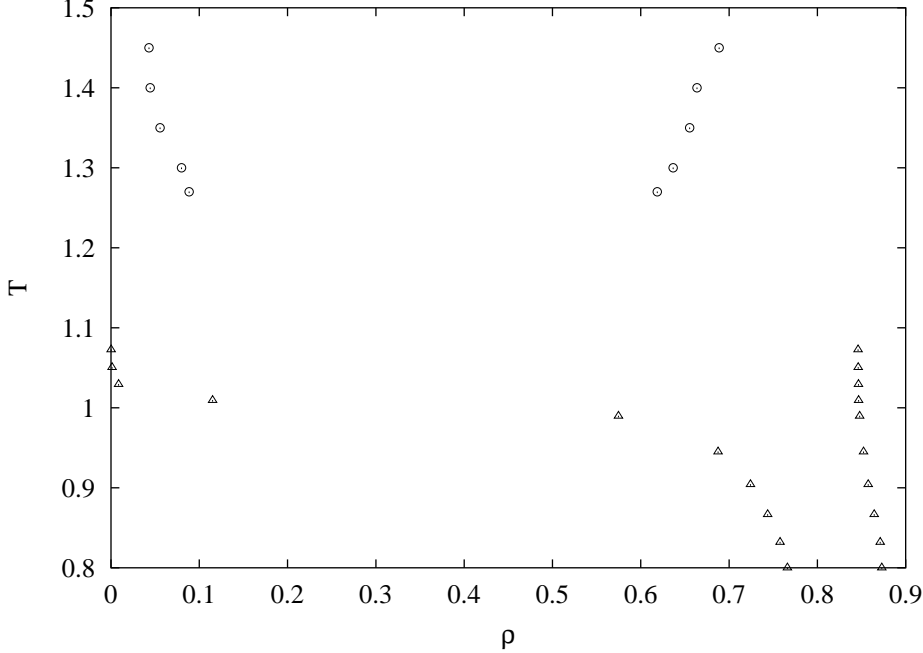


Figure 9: Phase diagram of the MLJ model including solvent-solute interactions. Interactions between the latter were mediated over the range $\lambda_s = 1.26$. Again 'x' denotes liquid-solidus line; '+' denotes fluid-fluid coexistence.

one can obtain an equivalent range in terms of λ , the parameter denoting the range in the square well system. We use the value $\lambda = 1.073$. To account for the effects of the effective hard-core diameter, we actually use $\lambda_s = 1.26$ for the solvent-solute interaction range. The values $\epsilon_w = -1$ and $\Delta S_w = -1.5$ were used as before to obtain an upside-down phase diagram.

To calculate the solid-fluid phase boundaries, we use a modified Gibbs-Duhem equation given by eq. 43. A coexistence point was calculated using free-energy methods and simulations of a coupled Einstein lattice. Isobaric-isothermal (NPT) simulations were performed in parallel for $N = 256$ particles on a periodic simulation cell to obtain the entire coexistence curve. Equilibration and production times were five million and ten million Monte Carlo steps, respectively.

We calculated the fluid-fluid coexistence curve using the Gibbs ensemble Monte Carlo method. Two physically separated, but thermodynamically connected, simulation cells are allowed to exchange particles and undergo volume displacements such that the total number of particles $N = N_1 + N_2$ and total volume $V = V_1 + V_2$ remain constant. Simulations were performed on an $N = 600$ particle system. Equilibration and production runs were fifty million and one hundred million Monte Carlo steps, respectively. Our results are shown in figure 9.

As can be seen from the figure, the phase diagram for this model with the particular parameters used is very similar to that for the square well model shown in figure 6.

7 Conclusion

The model presented in this paper takes into account the solvent contribution to the solute-solvent free energy of globular proteins in solution. The contribution depends on the parameters that describe the free energy of the solvent molecule change, ϵ_w and Δs_w . These parameters play the role of the solvent enthalpy and entropy change per solvent particle as the molecule goes from the bulk to the vicinity of the protein molecule. The solvent enthalpy and entropy change per solute particle upon changing from the fluid phase to the solid phase(parameters $\Delta H_{solvent}$ and $\Delta S_{solvent}$ from (1)) can be calculated as equal to ϵ_w and Δs_w times the difference of the average number of contacts per molecule in these two phases.

$$\Delta H_{solvent} = \epsilon_w (\langle n_c^{fluid} \rangle - \langle n_c^{solute} \rangle)$$

$$\Delta S_{solvent} = \Delta s_w (\langle n_c^{fluid} \rangle - \langle n_c^{solute} \rangle)$$

These relationships allow us to relate ϵ_w and Δs_w to the three cases of the solubility dependence described in the introduction - normal solubility dependence, retrograde solubility dependence and constant solubility (as in the case of apoferritin). All we need is the sign of the total enthalpy change ΔH . For the square well case, $\epsilon_w > -\epsilon_0/2$ is a condition for ΔH being negative and therefore the solubility curve being normal. If the range of attraction is short this qualitatively describes the lysozyme phase diagram. The condition $\epsilon_w < -\epsilon_0/2$ is a condition for ΔH being positive and therefore the solubility curve being retrograde. This corresponds to the case of the HbC solubility curve (fig. 1). Indeed we can see that the liquidus line in the figure 6 has qualitatively the same behavior as the HbC solubility curve. If $\epsilon_w \cong \epsilon/2$, so that the enthalpy change is small, then the solubility curve is almost vertical, with the sign of the slope determined by the sign of the enthalpy change.

The advantage of this simplified model is that in the particular case of the square well, with the particle-particle range of interaction equal to the width of the shell region around the particle, one can obtain the phase diagram by a mapping of the square well phase diagram without solvent. Therefore

one doesn't have to perform Monte Carlo simulations or theoretical approximations to obtain the phase diagram for the model with solvent.

The exact mapping is also possible for the hard sphere model with solvent. In this case $\epsilon_0 = 0$. The hard sphere case is interesting in two aspects. First, one can obtain an exact mapping procedure for any solvent-solute interaction. Second, the hard sphere interaction doesn't include any initial solvent contribution (unlike the case with an effective solute-solute interaction). This can be the case of noninteracting neutral colloidal particles in the solvent. If we put such particles into water, the hydrogen bonds break and rearrange, as explained in the introduction and in [1]. Therefore we can use the MLG model to get solvent parameters ϵ_w and Δs_w . We can consider the hard sphere interaction to be a square well with $\epsilon_0 = 0$ and $\lambda = \lambda_s$. Then using a mapping curve as in the figure 3 (the one with $\epsilon_0 = 0$) we can obtain the phase diagram of the neutral, noninteracting spherical particles in water. If the critical temperature of the square well system with a range of interaction equal to λ_s intersects the mapping curve (fig. 3), the colloidal system has a closed loop type phase diagram (fig 7 with $\epsilon_0 = 0$). As the value of λ_s decreases (the size of the particle increases), the fluid-fluid coexistence curve shrinks and disappears. So larger noninteracting particles don't have a fluid-fluid phase separation in this model. However, if the particles starts to interact, the mapping curve lowers (fig 3) and phase separation may occur again.

For the case of constant solvent parameters we can have either an upper critical point with a normal solubility dependence, or a lower critical point with a retrograde solubility dependence. The temperature dependent parameters allow us to have a combination of these behaviors. A natural way to derive the temperature dependent solvent parameters for water is to use the MLG model. This model, together with our solvent-solute interaction, has closed loop phase diagrams, similar to [1].

8 Acknowledgements

This work was supported by NSF grant DMR-0302598. One of us (A.S.) wishes to acknowledge the support and hospitality of the Theoretical Division of the Los Alamos National Laboratory, and a second (D.S.R.) wishes to acknowledge the support of the German Fulbright Commission and to thank the Helmholtz Institute for Radiation and Nuclear Physics of the University of Bonn, for the use of their

computing facilities.

References

- [1] S. Moelbert and P. De Los Rios. Hydrophobic Interaction Model for Upper and Lower Critical Solution Temperatures. *Macromolecules*, 36:5845, 2003.
- [2] A. George and W. W. Wilson. Predicting protein crystallization from a dilute solution property. *Acta Cryst. D*, 50:361, 1994.
- [3] C. F. Zukoski and D. F. Rosenbaum. Protein interactions and crystallization. *J. Cryst. Growth*, 169:752, 1996.
- [4] Siu-Tung Yau P. G. Vekilov, Angela R. Feeling-Taylor and Dimiter Petsev. Solvent entropy contribution to the free energy of protein crystallization. *Acta Cryst.D*, 58:1611, 2002.
- [5] A. Ben-Naim. *Water and Aqueous Solutions: Introduction to a Molecular Theory*. Plenum Press, New York, 1974.
- [6] H. S. Frank and M. W. Evans. Free Volume and Entropy in Condensed Systems. *J. Chem. Phys.*, 13:597, 1945.
- [7] M. Yaacobi and A. Ben-Naim. Solvophobic Interactions. *J. Phys. Chem.*, 74:175, 1974.
- [8] P. L. Privalov and S. J. Grill. Stability of Protein Structure and Hydrophobic Interaction. *Adv. Protein Chem.*, 39:191, 1988.
- [9] N. S. A. Davies and R. D. Gillard. Solubility loop of nicotine:water. *Trans. Met. Chem.*, 25:628, 2000.
- [10] D. S. Soane Y. C. Bae, S. M. Lambert and J. M. Prausnitz. Cloud-point curves of polymer solutions from thermo-optical measurements. *Macromolecules*, 24:4403, 1991.
- [11] H. G. Schild and D. A. Tirrell. Microcalorimetric detection of lower critical solution temperature in aqueous polymer solutions. *J. Phys. Chem.*, 94:4352, 1990.

- [12] R. O. R. Costa and R. F. S. Freitas. Phase Behavior of poly(N-isopropylacrylamide) in binary aqueous solutions . *Polymer*, 43:5879, 2002.
- [13] P. L. San Biagio and M. U. Palma. Spinodal lines and flory-huggins free-energies for solution of human hemoglobins hbs and hba. *Biophys. J.*, 60:508, 1991.
- [14] A. G. Phipps G. K. Christopher and R. J. Gray. Time-dependent solubility of selected proteins. *J. Cryst. Growth*, 191:820, 1998.
- [15] X.-J. Wang J. Lu and C.-B. Ching. Batch crystallization of soluble proteins: effect of precipitant, temperature and additive. *Prog. Cryst. Growth Charact.*, 45:201, 2002.
- [16] D. Costa G. Pellicane and C. Caccamo. Phase coexistence in a DLVO model of globular protein solutions. *J. Phys. Condens. Matter*, 15:375, 2003.
- [17] O. Galkin D. N. Petsev, X. Wu and P. G. Vekilov. Thermodynamic Functions of Concentrated Protein Solutions from Phase Equilibria. *J. Chem. Phys.*, 107:3921, 2003.
- [18] M. Kondo M. L. Broide J. Pande O. Ogun C. R. Berland, G. M. Thurston and G. B. Benedek. Solid-liquid phase boundaries of lens protein solutions. *Proc. Natl. Acad. Sci., USA*, 89:1214, 1992.
- [19] P. R. T. ten Wolde and D. Frenkel. Enhancement of protein crystal Nucleation by critical density fluctuation. *Science*, 277:1975, 1997.
- [20] F. N. Braun. Adhesion and liquid-liquid phase separation in globular protein solutions. *J. Chem. Phys.*, 116:6826, 2003.
- [21] N. Muller. Search for a Realistic View of Hydrophobic Effect. *Acc. Chem. Res.*, 23:23, 1990.
- [22] B. Lee and G. Graziano. A Two-State Model of Hydrophobic Hydration That Produces Compensating Enthalpy and Entropy Changes. *J. Am. Chem. Soc.*, 118:5163, 1996.
- [23] S. Moelbert. The Hydrophobic Interaction, PhD Thesis.
- [24] Brilliantov. Effective magnetic Hamiltonian and Ginzburg criterion for fluids. *Phys. Rev. E*, 58:2628, 1998.

- [25] D. Chandler H. C. Andersen and J. D. Weeks. Roles of repulsive and attractive forces in liquids: The optimized random phase approximation. *J. Chem. Phys.*, 56:3812, 1972.
- [26] D. A. Kofke. Gibbs-Duhem Integration: A New Method for Direct Evaluation of Phase Coexistence by Molecular Simulation. *Mol. Phys.*, 78:1331, 1993.
- [27] D. A. Kofke. Direct evaluation of phase coexistence by molecular simulation via integration along the saturation line. *J. Chem. Phys.*, 98:4149, 1993.